ASYMPTOTIC ENERGIES AND QED SHIFTS FOR THE RYDBERG STATES OF HELIUM

G.W.F. Drake
Department of Physics, University of Windsor
Windsor, Ontario, Canada N9B 3P4[1]

ABSTRACT

This paper reviews progress that has been made in obtaining essentially exact solutions to the nonrelativistic three-body problem for helium by a combination of variational and asymptotic expansion methods. The calculation of relativistic and quantum electrodynamic corrections by perturbation theory is discussed, and in particular, methods for the accurate calculation of the Bethe logarithm part of the electron self energy are presented. As an example, the results are applied to the calculation of isotope shifts for the short-lived 'halo' nucleus ^{6}He relative to ^{4}He in order to determine the nuclear charge radius of ^{6}He from high precision spectroscopic measurements carried out at the Argonne National Laboratory. The results demonstrate that the high precision that is now available from atomic theory is creating new opportunities to create novel measurement tools, and helium, along with hydrogen, can be regarded as a fundamental atomic system whose spectrum is well understood for all practical purposes.

INTRODUCTION

The goal of the work presented here is to obtain essentially exact theoretical values for the energy levels for the entire singly excited spectrum of helium and its isotopes, including all terms up to order α^3 Ry, where $\alpha \simeq 1/137.035\,999\,11(46)$ is the fine structure constant. The achievement of this goal requires accurate nonrelativistic eigenvalues, relativistic corrections of order α^2 Ry, and quantum electrodynamic corrections of order α^3 Ry. Recent advances over the past several years now make it possible to obtain solutions to the quantum mechanical three- and four-body problem that are essentially exact for all practical purposes, at least in the nonrelativistic limit. The calculation of the lowest order α^2 Ry relativistic corrections is then straight forward, but the calculation of the QED corections (especially the Bethe logarithm) has remained a long- standing problem in atomic physics. This last problem has also now been solved, as will be described in this paper, thereby opening the way to complete calculations up to order α^3 Ry.

On the experimental side, there is a large body of high precision data available for comparison. The particular significance in relation to the present work is that the theoretical uncertainty in the D-states is now so small that their energies can be taken as absolute points of reference. The measured transition frequencies to the lower-lying S- and P-states can then be used to determine the absolute ionization energies of these states (see Drake and Martin [1]), and from this the QED energy shifts can be determined.

The second goal of this work is to use the comparison between theory and experiment for the isotope shift to determine the nuclear charge radius for various isotopes of helium. There is now considerable interest in using this method to measure the nuclear charge radii of of exotic 'halo' nuclei such as ^{6}He and ^{8}He first discovered by Tanihata [2]. As will be seen, this technique provides a unique measurement tool to perform nuclear size measurements that cannot be done in any other way.

[1]E-mail: GDrake@uwindsor.ca

Table 1: Contributions to the energy and their orders of magnitude in terms of Z, $\mu/M = 1.370\,745\,624 \times 10^{-4}$, and $\alpha^2 = 0.532\,513\,5450 \times 10^{-4}$.

Contribution	Magnitude
Nonrelativistic energy	Z^2
Mass polarization	$Z^2\mu/M$
Second-order mass polarization	$Z^2(\mu/M)^2$
Relativistic corrections	$Z^4\alpha^2$
Relativistic recoil	$Z^4\alpha^2\mu/M$
Anomalous magnetic moment	$Z^4\alpha^3$
Hyperfine structure	$Z^3 g_I \mu_0^2$
Lamb shift	$Z^4\alpha^3 \ln\alpha + \cdots$
Radiative recoil	$Z^4\alpha^3(\ln\alpha)\mu/M$
Finite nuclear size	$Z^4\langle \bar{r}_c/a_0\rangle^2$

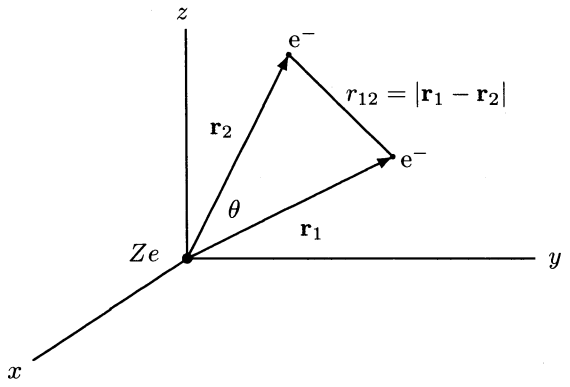

Figure 1: Coordinate system for a helium atom with the nucleus at the origin.

THEORETICAL BACKGROUND

Table 1 summarizes the various contributions to the energy, expressed as a double expansion in powers of $\alpha \simeq 1/137.036$ and the electron reduced mass ratio $\mu/M \simeq 10^{-4}$. Since all the lower-order terms can now be calculated to very high precision, including the QED terms of order α^3 Ry, the dominant source of uncertainty comes from the QED corrections of order α^4 Ry or higher. The comparison between theory and experiment is therefore sensitive to these terms. For the isotope shift, the QED terms independent of μ/M cancel out, and so it is only the radiative recoil terms of order $\alpha^4\mu/M \simeq 10^{-12}$Ry ($\sim$ 10 kHz) that contribute to the uncertainty. Since this is much less than the finite nuclear size correction of about 1 MHz, the comparison between theory and experiment clearly provides a means to determine the nuclear size.

Solution to the Nonrelativistic Schrödinger Equation

The starting point for the calculation is to find accurate solutions to the Schrödinger equation for helium. Considering first the case of infinite nuclear mass, the equation in atomic units is given by

$$\left(-\frac{1}{2}\nabla_1^2 - \frac{1}{2}\nabla_2^2 - \frac{Z}{r_1} - \frac{Z}{r_2} + \frac{1}{r_{12}}\right)\Psi(\mathbf{r}_1,\mathbf{r}_2) = E\Psi(\mathbf{r}_1,\mathbf{r}_2) \tag{1}$$

The usual methods of theoretical atomic physics, such as the Hartree-Fock approximation or configuration interaction methods, are not capable of yielding results of spectroscopic accuracy. For this reason, specialized methods have been developed. As long ago as 1929, Hylleraas suggested expanding the wave function in an explicitly correlated variational basis set of the form

$$\Psi(\mathbf{r}_1,\mathbf{r}_2) = \sum_{i,j,k} a_{ijk}\, r_1^i r_2^j r_{12}^k\, e^{-\alpha r_1 - \beta r_2}\, \mathcal{Y}^M_{l_1 l_2 L}(\hat{\mathbf{r}}_1,\hat{\mathbf{r}}_2) \tag{2}$$

where $r_{12} = |\mathbf{r}_1 - \mathbf{r}_2|$ is the interelectronic separation (see Fig. 1). The coefficients a_{ijk} are linear variational parameters, and α and β are nonlinear variational coefficients that set the distance scale for the wave function. The usual strategy is to include all powers such that $i + j + k \leq \Omega$ (a so-called Pekeris shell), where Ω is an integer. The inclusion of powers of r_{12}, and especially the odd powers, makes the basis set rapidly convergent as Ω increases. The basis set is proveably complete in the limit $\Omega \to \infty$ [3].

For states of higher angular momentum L, the quantity $\mathcal{Y}^M_{l_1 l_2 L}(\hat{\mathbf{r}}_1,\hat{\mathbf{r}}_2)$ denotes a vector-coupled product of spherical harmonics, and the basis set includes a summation over the possible integer values of l_1 and l_2 (with l_2 constrained to be $l_2 = L - l_1$) such that $l_1 \leq L/2$. In addition, the nonlinear parameters α and β are separately optimized for each set of angular momentum terms, and, as discussed in Refs. [4, 5, 6], it is desirable further to 'double' the basis set so that each set of powers $\{i, j, k\}$ is included two (or more [7]) times with different values of α and β. For sufficiently large basis sets, the doubling is very important because it helps to preserve the numerical stability of the wave function, it gives improved accuracy for a given total size of basis set, and it avoids the disasterous loss of accuracy that normally sets in for variational calculations involving the higher-lying Rydberg states [4, 5, 6].

The principal computational steps are first to orthogonalize the χ_{ijk} basis set, and then to diagonalize the Hamiltonian matrix $\mathbf{H}$ in the orthogonalized basis set so as to satisfy the Rayleigh-Schrödinger variational principle

$$\delta \int \Psi\,(H - E)\,\Psi\, d\tau = 0. \tag{3}$$

Finally, a complete optimization is performed with respect to variations in the αs and βs so as to minimize the energy.

For high precision calculations, and especially for the istope shift, it is necessary to include also the motion of the nucleus in the center-of-mass (CM) frame. A transformation to CM plus relative coordinates yields the additional $-(\mu/M)\nabla_1 \cdot \nabla_2$ mass polarization term in the modified Hamiltonian

$$H = -\frac{1}{2}\nabla_1^2 - \frac{1}{2}\nabla_2^2 - \frac{Z}{r_1} - \frac{Z}{r_2} + \frac{1}{r_{12}} - \frac{\mu}{M}\nabla_1 \cdot \nabla_2 \tag{4}$$

in reduced mass atomic units e^2/a_μ, where $a_\mu = (m_e/\mu)a_0$ is the reduced mass Bohr radius, and $\mu = m_e M/(m_e + M)$ is the electron reduced mass, M is the nuclear mass, and $a_0 = \hbar^2/m_e e^2$ is the Bohr radius. The mass polarization term can be treated either by including it as a perturbation (up to second-order),

Table 2: Convergence study for the ground state of helium (infinite nuclear mass case) [7]. N is the number of terms in the 'triple' basis set.

Ω	N	$E(\Omega)$	$R(\Omega)$
8	269	−2.903 724 377 029 560 058 400	
9	347	−2.903 724 377 033 543 320 480	
10	443	−2.903 724 377 034 047 783 838	7.90
11	549	−2.903 724 377 034 104 634 696	8.87
12	676	−2.903 724 377 034 116 928 328	4.62
13	814	−2.903 724 377 034 119 224 401	5.35
14	976	−2.903 724 377 034 119 539 797	7.28
15	1150	−2.903 724 377 034 119 585 888	6.84
16	1351	−2.903 724 377 034 119 596 137	4.50
17	1565	−2.903 724 377 034 119 597 856	5.96
18	1809	−2.903 724 377 034 119 598 206	4.90
19	2067	−2.903 724 377 034 119 598 286	4.44
20	2358	−2.903 724 377 034 119 598 305	4.02
Extrapolation	∞	−2.903 724 377 034 119 598 311(1)	
Korobov [11]	5200	−2.903 724 377 034 119 598 311 158 7	
Korobov extrap.	∞	−2.903 724 377 034 119 598 311 159 4(4)	
Schwartz [12]	10259	−2.903 724 377 034 119 598 311 159 245 194 404 4400	
Schwartz extrap.	∞	−2.903 724 377 034 119 598 311 159 245 194 404 446	
Goldman [13]	8066	−2.903 724 377 034 119 593 82	
Bürgers *et al.* [14]	24 497	−2.903 724 377 034 119 589(5)	
Baker *et al.* [15]	476	−2.903 724 377 034 118 4	

or by including it explicitly in the Hamiltonian. The latter procedure is simpler and more direct, and the coefficient of the second-order term can still be extracted by differencing [4, 6]. A general method for the decomposition of this equation was developed many years ago by Bhatia and Temkin [8], and the effects of mass polarization studied by Bhatia and Drachman [9] for a range of values of μ/M. These authors have also extended the calculation of the second-order mass polarization term for several low-lying states to the He-like ions [10].

As an example, Table 2 shows a convergence study for the very well studied case of the ground state of helium [7]. The quantity R in the last column is the ratio of successive differences between the energies. A constant or slowly changing value of R indicates smooth convergence, and allows a reliable extrapolation to $\Omega \to \infty$. The results clearly indicate that convergence to 20 or more figures can be readily obtained, using conventional quadruple precision (32 decimal digit) arithmetic in FORTRAN. The very large calculation by Schwartz [12], using 104-digit arithmetic, provides a benchmark for comparison.

ASYMPTOTIC EXPANSION METHOD

Richard Drachman is largely responsible for the development of the asymptotic expansion method for helium, based on a core polarization model [16, 17, 18, 19, 20, 21]. It provides a means to give a physical interpretation and meaning to these long strings of significant figures for the nonrelativistic eigenvalues, at least in the limit

Table 3: Variational energies for the $n = 10$ singlet and triplet states of helium.

State	Singlet	Triplet
10 S	−2.005 142 991 747 919(79)	−2.005 310 794 915 611 3(11)
10 P	−2.004 987 983 802 217 9(26)	−2.005 068 805 497 706 7(30)
10 D	−2.005 002 071 654 256 81(75)	−2.005 002 818 080 228 84(53)
10 F	−2.005 000 417 564 668 80(11)	−2.005 000 421 686 604 88(26)
10 G	−2.005 000 112 764 318 746(22)	−2.005 000 112 777 003 317(21)
10 H	−2.005 000 039 214 394 532(17)	−2.005 000 039 214 417 416(17)
10 I	−2.005 000 016 086 516 1947(3)	−2.005 000 016 086 516 2194(3)
10 K	−2.005 000 007 388 375 8769(0)	−2.005 000 007 388 375 8769(0)

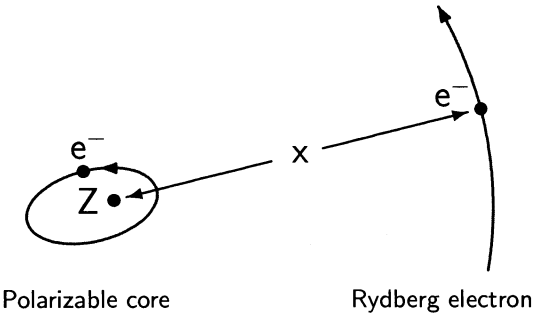

Figure 2: Illustration of the physical basis for the asymptotic expansion method in which the Rydberg electron moves in the field generated by the polarized core.

of large L. As shown in Table 3 for the list of states with $n = 10$, the singlet-triplet splitting goes exponentially to zero with increasing L, so that for $L = 7$ (K-states), the splitting is no longer visible to the 20 figure accuracy of the calculations. This indicates that the Rydberg electron can be treated as a distinguishable particle interacting with a polarizable core consisting of the nucleus and the inner $1s$ electron. The leading figures in the energies correspond to the simple screened hydrogenic energy

$$\begin{aligned} E &= -2 - \frac{1}{2n^2} + \cdots \\ &= -2.005 \cdots \end{aligned} \tag{5}$$

for $n = 10$. Here, the -2 is the energy of the inner $1s$ electron with nuclear charge $Z = 2$, and the $-1/(2n^2)$ is the energy of the outer Rydberg electron for the screened nuclear charge $Z = 1$. For the 10K state, this simple calculation accounts for the leading eight significant figures in the energy, and so all the interesting physics is contained in the figures that come after the eighth.

Our objective now is to see how much of this interesting physics after the eighth figure in the energy (for K-states) can be understood in terms of the asymptotic expansion method. Figure 2 illustrates the physical basis for the core polarization model. Letting x denote the radial coordinate of the Rydberg electron, it moves in the asymptotic potential

$$V(x) = -\frac{Z-1}{x} + \Delta V(x) \tag{6}$$

Table 4: Asymptotic expansion for the energy of the 1s10k state of helium.

Quantity	Value
$-Z^2/2$	–2.000 000 000 000 000 00
$-1/(2n^2)$	–0.005 000 000 000 000 00
$c_4\langle r^{-4}\rangle$	–0.000 000 007 393 341 95
$c_6\langle r^{-6}\rangle$	0.000 000 000 004 980 47
$c_7\langle r^{-7}\rangle$	0.000 000 000 000 278 95
$c_8\langle r^{-8}\rangle$	–0.000 000 000 000 224 33
$c_9\langle r^{-9}\rangle$	–0.000 000 000 000 002 25
$c_{10}\langle r^{-10}\rangle$	0.000 000 000 000 003 73
Second order	–0.000 000 000 000 070 91
Total	–2.005 000 007 388 376 30(74)
Variational	–2.005 000 007 388 375 8769(0)
Difference	–0.000 000 000 000 000 42(74)
	$\simeq$ 3 Hz

where $Z-1$ is the screened nuclear charge, and the polarization potential due to the core is

$$\Delta V(x) = -\frac{c_4}{x^4} - \frac{c_6}{x^6} - \frac{c_7}{x^7} - \frac{c_8}{x^8} - \frac{c_9}{x^9} - \frac{c_{10}}{x^{10}} + \cdots \tag{7}$$

For example, $c_4 = \alpha_1/2$, where α_1 is the dipole polarizability of the core, and the other coefficients are similarly related to the higher multipole moments of the core. Since the core is a one-electron hydrogenic problem, all the c_i coefficients can be calculated exactly as simple rational fractions [6]. For example, $\alpha_1 = 9/(2Z^4)\, a_0^3$.

The screened hydrogenic energy is then given by

$$\Delta E_{nL} = -\frac{(Z-1)^2}{2n^2} + \langle\chi_0 \mid \Delta V(x) \mid \chi_0\rangle + \langle\chi_0 \mid \Delta V(x) \mid \chi_1\rangle \tag{8}$$

where $\mid \chi_1\rangle$ is first-order perturbation correction to $\mid \chi_0\rangle$ due to $\Delta V(x)$; i.e. it satisfies the perturbation equation [22]

$$[h_0(x) - e_0] \mid \chi_1\rangle + \Delta V(x) \mid \chi_0\rangle = \mid \chi_0\rangle\langle\chi_0 \mid \Delta V(x) \mid \chi_0\rangle \tag{9}$$

Continuing with the example of $n = 10$, Table 4 lists the various contributions from the multipole expansion for the case $L = 7$, including the second-order term. The ± 3 Hz accuracy of the asymptotic expansion is more than sufficient for comparisons with experiment. For low L, the asymptotic expansion is much less accurate because the series must be truncated when the terms start increasing. Indeed the expectation values $\langle 1/x^n\rangle$ diverge for $n > 2L+2$. However, the accuracy rapidly improves with increasing L, and there is clearly no need for direct variational calculations for $L > 7$.

Variational Basis Sets for Lithium

The same variational techniques can be applied to lithium and other three-electron atomic systems. In this case, the terms in the Hylleraas correlated basis set have the form

$$r_1^{j_1}\, r_2^{j_2}\, r_3^{j_3}\, r_{12}^{j_{12}}\, r_{23}^{j_{23}}\, r_{31}^{j_{31}}\, e^{-\alpha r_1 - \beta r_2 - \gamma r_3}\, \mathcal{Y}^{LM}_{(\ell_1\ell_2)\ell_{12},\ell_3}(\mathbf{r}_1, \mathbf{r}_2, \mathbf{r}_3)\, \chi_1\,, \tag{10}$$

where $\mathcal{Y}^{LM}_{(\ell_1\ell_2)\ell_{12},\ell_3}$ is again a vector-coupled product of spherical harmonics, and χ_1 is a spin function with spin angular momentum 1/2. As for helium, the usual strategy is to include all terms from (10) such that

$$j_1 + j_2 + j_3 + j_{12} + j_{23} + j_{31} \quad \leq \quad \Omega\,, \tag{11}$$

and study the eigenvalue convergence as Ω is progressively increased. The lithium problem is much more difficult than helium both because the integrals over fully correlated wave functions are more difficult, and because the basis set grows much more rapidly with increasing Ω. Nevertheless, there has been important progress in recent years [23, 24, 25], and results of spectroscopic accuracy can be obtained for the low-lying states.

Bhatia and Drachman have also made important progress in applying the asymptotic expansion methods to the Rydberg states of lithium [26, 27, 28]. The calculations in this case are more difficult because the 'polarizable core' now consists of the nucleus and two $1s$ electrons, and so its multipole moments cannot be calculated analytically.

RELATIVISTIC CORRECTIONS

This section briefly summarizes the lowest-order relativistic corrections of order α^2 Ry, and the relativistic recoil corrections of order $\alpha^2\mu/M$ Ry. The well-known terms in the Breit interaction [29] (including for convenience the anomalous magnetic moment terms of order α^3 Ry) give rise to the first-order perturbation correction

$$\Delta E_{\rm rel} \quad = \quad \langle \Psi_J | H_{\rm rel} | \Psi_J \rangle\,, \tag{12}$$

where Ψ_J is a nonrelativistic wave function for total angular momentum $\mathbf{J} = \mathbf{L} + \mathbf{S}$ and $H_{\rm rel}$ is defined by (in atomic units)

$$\begin{aligned} H_{\rm rel} \quad = \quad & \left(\frac{\mu}{m_{\rm e}}\right)^4 B_1 + \left(\frac{\mu}{m_{\rm e}}\right)^3 \Bigg[B_2 + B_4 + B_{\rm so} + B_{\rm soo} + B_{\rm ss} + \frac{m_{\rm e}}{M}(\tilde{\Delta}_2 + \tilde{\Delta}_{\rm so}) \\ & + \gamma \left(2B_{\rm so} + \frac{4}{3} B_{\rm soo} + \frac{2}{3} B^{(1)}_{3e} + 2B_5 \right) + \gamma \frac{m_{\rm e}}{M} \tilde{\Delta}_{\rm so} \Bigg]\,. \end{aligned} \tag{13}$$

with $\gamma = \alpha/(2\pi)$. The factors of $(\mu/m_{\rm e})^4 = (1 - \mu/M)^4$ and $(\mu/m_{\rm e})^3 = (1 - \mu/M)^3$ arise from the mass scaling of each term in the Breit interaction, while the terms $\tilde{\Delta}_2$ and $\tilde{\Delta}_{\rm so}$ are dynamical corrections arising from the transformation of the Breit interaction to CM plus relative coordinates [30]. These latter terms are often not included in atomic structure calculations, but they make an important contribution to the isotope shift. The explicit expressions for the spin-independent operators are

$$B_1 = \frac{\alpha^2}{8}(p_1^4 + p_2^4) \tag{14}$$

$$B_2 = -\frac{\alpha^2}{2}\left(\frac{1}{r_{12}} \mathbf{p}_1 \cdot \mathbf{p}_2 + \frac{1}{r_{12}^3} \mathbf{r}_{12} \cdot (\mathbf{r}_{12} \cdot \mathbf{p}_1) \mathbf{p}_2 \right) \tag{15}$$

$$B_4 = \alpha^2 \pi \left(\frac{Z}{2} \delta(\mathbf{r}_1) + \frac{Z}{2} \delta(\mathbf{r}_2) - \delta(\mathbf{r}_{12}) \right) \tag{16}$$

and the spin-dependent terms are

$$B_{\rm so} = \frac{Z\alpha^2}{4} \left[\frac{1}{r_1^3} (\mathbf{r}_1 \times \mathbf{p}_1) \cdot \boldsymbol{\sigma}_1 + \frac{1}{r_2^3} (\mathbf{r}_2 \times \mathbf{p}_2) \cdot \boldsymbol{\sigma}_2 \right] \tag{17}$$

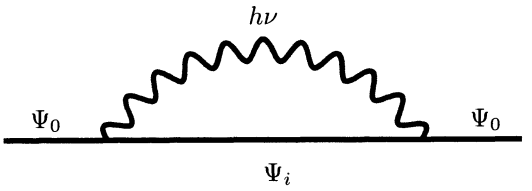

Figure 3: Feynman diagram for the electron self energy.

$$B_{\rm soo} = \frac{\alpha^2}{4}\left[\frac{1}{r_{12}^3}\mathbf{r}_{12}\times\mathbf{p}_2\cdot(2\boldsymbol{\sigma}_1+\boldsymbol{\sigma}_2) - \frac{1}{r_{12}^3}\mathbf{r}_{12}\times\mathbf{p}_1\cdot(2\boldsymbol{\sigma}_2+\boldsymbol{\sigma}_1)\right] \tag{18}$$

$$B_{\rm ss} = \frac{\alpha^2}{4}\left[-\frac{8}{3}\pi\delta(\mathbf{r}_{12}) + \frac{1}{r_{12}^3}\boldsymbol{\sigma}_1\cdot\boldsymbol{\sigma}_2 - \frac{3}{r_{12}^3}(\boldsymbol{\sigma}_1\cdot\mathbf{r}_{12})(\boldsymbol{\sigma}_2\cdot\mathbf{r}_{12})\right] \tag{19}$$

Finally, the relativistic recoil terms are [30]

$$\begin{aligned}\tilde{\Delta}_2 &= -\frac{Z\alpha^2}{2}\left\{\frac{1}{r_1}(\mathbf{p}_1+\mathbf{p}_2)\cdot\mathbf{p}_1 + \frac{1}{r_1^3}br_1\cdot[\mathbf{r}_1\cdot(\mathbf{p}_1+\mathbf{p}_2)]\mathbf{p}_1\right.\\ &\left.+\frac{1}{r_2}(\mathbf{p}_1+\mathbf{p}_2)\cdot\mathbf{p}_2 + \frac{1}{r_2^3}br_2\cdot[\mathbf{r}_2\cdot(\mathbf{p}_1+\mathbf{p}_2)]\mathbf{p}_2\right\}\end{aligned} \tag{20}$$

$$\tilde{\Delta}_{\rm so} = \frac{Z\alpha^2}{2}\left(\frac{1}{r_1^3}\mathbf{r}_1\times\mathbf{p}_2\cdot\boldsymbol{\sigma}_1 + \frac{1}{r_2^3}\mathbf{r}_2\times\mathbf{p}_1\cdot\boldsymbol{\sigma}_2\right) \tag{21}$$

It is then a relatively straight forward matter to calculate accurate expectation values for these operators. Also, asymptotic expansions have been derived for the matrix elements and compared with the direct variational calculations, as discussed in Ref. [6].

QED CORRECTIONS

For a many-electron atom, the total QED shift of order α^3 Ry consists of two parts—an electron-nucleus part $E_{\rm L,1}$ (the Kabir-Salpeter term [31]), and an electron-electron term $E_{\rm L,2}$ originally obtained by Araki [32] and Sucher [33]. The $E_{\rm L,2}$ term is relatively small and stright-forward to calculate. The principal computational challenges come from the $E_{\rm L,1}$ term given by (in atomic units)

$$E_{L,1} = \frac{4}{3}Z\alpha^3\langle\delta(\mathbf{r}_1)+\delta(\mathbf{r}_2)\rangle\left[\ln\alpha^{-2} - \beta(1s n\ell) + \frac{19}{30}\right] \tag{22}$$

where $\beta(1sn\ell)$ is the two-electron Bethe logarithm arising from the emission and re-absorption of a virtual photon (see Fig. 3). It is the logarithmic remainder after mass renormalization, and is defined by

$$\beta(1sn\ell) = \frac{\mathcal{N}}{\mathcal{D}} = \frac{\sum_i |\langle\Psi_0|\mathbf{p}_1+\mathbf{p}_2|i\rangle|^2(E_i-E_0)\ln|E_i-E_0|}{\sum_i |\langle\Psi_0|\mathbf{p}_1+\mathbf{p}_2|i\rangle|^2(E_i-E_0)} \tag{23}$$

The foregoing equations are virtually identical to the corresponding one-electron (hydrogenic) case, except that there the δ-function matrix elements can be replaced by their hydrogenic value

$$\langle\delta(\mathbf{r}_1)+\delta(\mathbf{r}_2)\rangle \to Z^3/(\pi n^3) \tag{24}$$

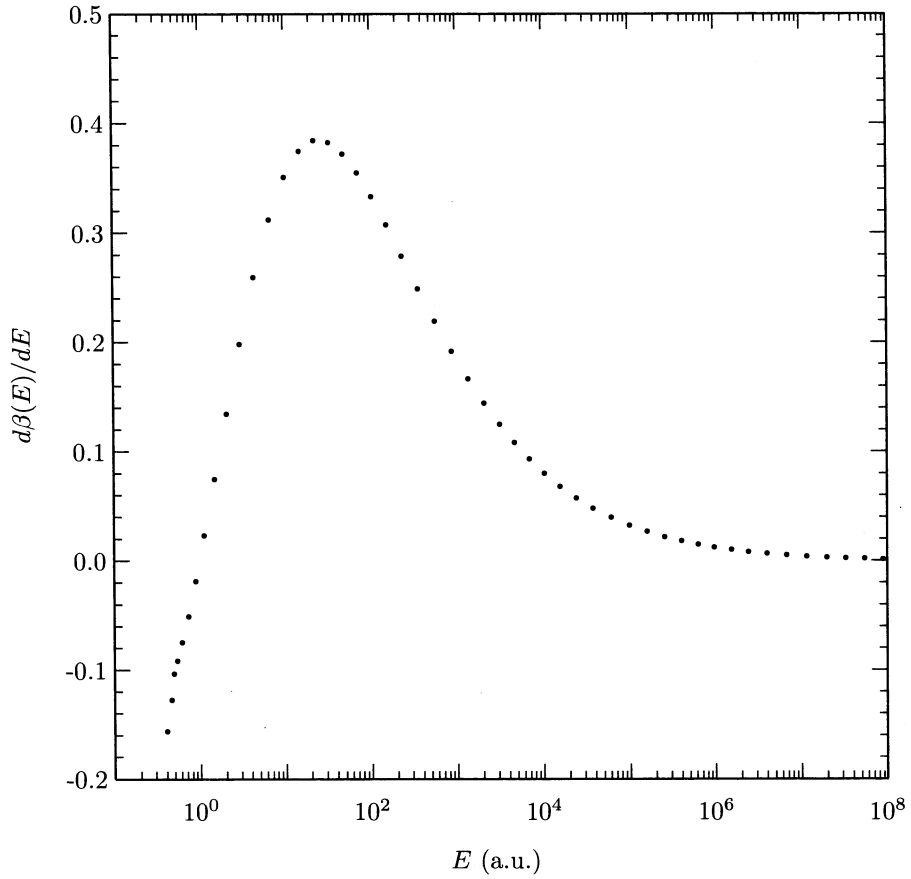

Figure 4: Differential contributions to the Bethe logarithm for the ground state of hydrogen. Each point represents the contribution from one pseudostate.

The sum in the denominator of (23) can be completed by closure with the result

$$\mathcal{D} = \langle\Psi_0|\mathbf{p}(H - E_0)\mathbf{p}|\Psi_0\rangle = 2\pi Z\langle\delta(\mathbf{r}_1) + \delta(\mathbf{r}_2)\rangle \tag{25}$$

where $\mathbf{p} = \mathbf{p}_1 + \mathbf{p}_2$. The numerator is much more difficult to calculate because the sum over intermediate states (including an integration over the continuum) cannot be performed analytically, and a sum over pseudostates nearly diverges at high energies. Schwartz [34] transformed the numerator to read

$$\mathcal{N} = \lim_{K\to\infty}\left(-K\langle\Psi_0|\mathbf{p}\cdot\mathbf{p}|\Psi_0\rangle + \mathcal{D}\ln(K) + \int_0^K k\,dk\langle\Psi_0|\mathbf{p}(H - E_0 + k)^{-1}\mathbf{p}|\Psi_0\rangle\right) \tag{26}$$

However, this is slowly convergent, and expensive in computer time since a matrix diagonalization must be performed at each integration point. Despite this, results of useful accuracy for the lowest-lying S- and P-states have been obtained by this method in Refs. [35], [36], and [37].

An alternative method based on a discrete variational representation of the continuum in terms of pseudostates has been developed by Drake and Goldman [38]. The method is simplest to explain for the case of hydrogen. The key idea is to define a variational basis set containing a huge range of distance scales

Table 5: Convergence of the Bethe logarithm $\beta(1s) = \ln(k_0/\mathrm{R}_\infty)$ for hydrogen. $\mathrm{R}_\infty = 3.289\,841\,960\,360(22) \times 10^9$ MHz is the Rydberg constant.

Ω	N	$\beta(1s)$	Differences	Ratios
2	3	2.73448191727230174149		
3	6	2.94877219077044909822	0.21429027349814735672	
4	10	2.97975301862169611861	0.03098082785124702039	6.917
5	15	2.98361449929795351803	0.00386148067625739942	8.023
6	21	2.98407183714911362800	0.00045733785116010997	8.443
7	28	2.98412247036420809592	0.00005063321509446792	9.032
8	36	2.98412792735460886871	0.00000545699040077279	9.279
9	45	2.98412849201006208099	0.00000056465545321228	9.664
10	55	2.98412854946585020174	0.00000005745578812075	9.828
11	66	2.98412855514977775545	0.00000000568392755370	10.108
12	78	2.98412855570645173753	0.00000000055667398208	10.211
13	91	2.98412855575986426711	0.00000000005341252957	10.422
14	105	2.98412855576496736061	0.00000000000510309350	10.467
15	120	2.98412855576544766988	0.00000000000048030928	10.625
16	136	2.98412855576549294823	0.00000000000004527834	10.608
17	153	2.98412855576549717245	0.00000000000000422422	10.719
18	171	2.98412855576549756974	0.00000000000000039729	10.633
19	190	2.98412855576549760688	0.00000000000000003714	10.697
20	210	2.98412855576549761038	0.00000000000000000351	10.594
Extrap.		2.98412855576549761075		

according to:

$$\chi_{i,j} = r^i \exp(-\alpha_j r)\cos(\theta), \tag{27}$$

with $j = 0, 1, \ldots, \Omega - 1$, $i = 0, 1, \ldots, \Omega - j - 1$, and

$$\alpha_j = \alpha_0 \times g^j, \quad g \simeq 10, \quad \alpha_0 \simeq 1\,. \tag{28}$$

Thus, each increase in Ω introduces another set of terms containing different powers of r, but with a distance scale $1/\alpha_j$ that is approximately a factor of 10 smaller than the previous one (a number close to 10 happens to be the variational optimum). For example, for p-states $\chi_{0,20} \simeq \exp(10^{20} r)\cos\theta$. As shown in Fig. 4, this has the effect of pushing the eigenvalue spectrum up to enormously high energies far above the few tens of atomic units that one would normally expect for a variational basis set. The number of elements is $N = \Omega(\Omega+1)/2$. One then follows the usual procedure of orthogonalizing the basis set, and then diagonalizing the Hamiltonian to generate a set of N pseudostates that can be summed over to calculate the Bethe logarithm.

As an example, for the ground $1s$ state of hydrogen, one would generate a set of pseudostates with p-symmetry, and then calculate the dipole transition integrals in Eq. (23). An additional trick to speed convergence is to include in the basis set terms that behave as r^{l-1} at the origin for pseudostates of angular momentum l. Such terms of course do not contribute to the exact wave functions of angular momentum l, but they do contribute to the effective Green's function that the sum over intermediate states represents (see Ref. [38] for further details). The results in Table 5 demonstrate that the Bethe logarithm calculated in this way converges to the known result for the $1s$ ground state of hydrogen to 20 figure accuracy. Figure 4 shows the differential contributions to the Bethe logarithm from each pseudostate. It is clear that extremely high energies are needed to capture the majority of the Bethe logarithm. The basis set has good numerical stability, and standard quadruple precision (32 decimal digit) arithmetic is sufficient for the example shown.

Table 6: Bethe logarithms $\ln(k_0/Z^2\mathrm{R}_\infty)$ for He-like atoms, from Ref. [38] (see also Ref. [39]).

State	$Z=2$	$Z=3$	$Z=4$	$Z=5$	$Z=6$
$1\ ^1$S	2.983 865 9(1)	2.982 624 558(1)	2.982 503 05(4)	2.982 591 383(7)	2.982 716 949(1)
$2\ ^1$S	2.980 118 275(4)	2.976 363 09(2)	2.973 976 98(4)	2.972 388 16(3)	2.971 266 29(2)
$2\ ^3$S	2.977 742 36(1)	2.973 851 679(2)	2.971 735 560(4)	2.970 424 952(5)	2.969 537 065(5)
$2\ ^1$P	2.983 803 49(3)	2.983 186 10(2)	2.982 698 29(1)	2.982 340 18(7)	2.982 072 79(6)
$2\ ^3$P	2.983 690 84(2)	2.982 958 68(7)	2.982 443 5(1)	2.982 089 5(1)	2.981 835 91(5)
$3\ ^1$S	2.982 870 512(3)	2.981 436 5(3)	2.980 455 81(7)	2.979 778 086(4)	2.979 289 8(9)
$3\ ^3$S	2.982 372 554(8)	2.980 849 595(7)	2.979 904 876(3)	2.979 282 037	2.978 844 34(6)
$3\ ^1$P	2.984 001 37(2)	2.983 768 943(8)	2.983 584 906(6)	2.983 449 763(6)	2.983 348 89(1)
$3\ ^3$P	2.983 939 8(3)	2.983 666 36(4)	2.983 479 30(2)	2.983 350 844(8)	2.983 258 40(4)
$4\ ^1$S	2.983 596 31(1)	2.982 944 6(3)	2.982 486 3(1)	2.982 166 154(3)	2.981 932 94(5)
$4\ ^3$S	2.983 429 12(5)	2.982 740 35(4)	2.982 291 37(7)	2.981 988 21(2)	2.981 772 015(7)
$4\ ^1$P	2.984 068 766(9)	2.983 961 0(2)	2.983 875 8(1)	2.983 813 2(1)	2.983 766 6(2)
$4\ ^3$P	2.984 039 84(5)	2.983 913 45(9)	2.983 828 9(1)	2.983 770 1(2)	2.983 727 5(2)
$5\ ^1$S	2.983 857 4(1)	2.983 513 01(2)	2.983 267 901(6)	2.983 094 85(5)	2.982 968 66(2)
$5\ ^3$S	2.983 784 02(8)	2.983 422 50(2)	2.983 180 677(6)	2.983 015 17(3)	2.982 896 13(2)
$5\ ^1$P	2.984 096 174(9)	2.984 038 03(5)	2.983 992 23(1)	2.983 958 67(5)	2.983 933 65(5)
$5\ ^3$P	2.984 080 3(2)	2.984 014 4(4)	2.983 968 9(4)	2.983 937 2(4)	2.983 914 07(6)

Bethe Logarithms for Helium and Lithium

The basis sets for helium and lithium are more complicated in detail but the principles are the same. In each case the Bethe logarithm comes almost entirely from virtual excitations of the inner $1s$ electron to p-states lying high in the photoionization continuum, and so the basis set must be extended to very short distances for this particle. The outer electrons are to a good approximation just spectators to these virtual excitations.

Results for the low-lying states of helium and the He-like ions are listed in Table 6 (see also Korobov [39]). In order to make the connection with the hydrogenic Bethe logarithm more obvious, the quantity tabulated is $\ln(k_0/Z^2\mathrm{R}_\infty)$. The effect of dividing by a factor of Z^2 is to reduce all the Bethe logarithms to approximately the same number $\beta(1s) = 2.984\,128\,556$ for the ground state of hydrogen. It is convenient to express the results in the form $\beta(1snL) = \beta(1s) + \Delta\beta(nL)/n^3$, where $\Delta\beta(nL)$ is a small number that tends to a constant at the series limit.

Because of the many contributions of Richard Drachman to the core polarization model and the asymptotic expansion method, it is especially appropriate for this volume to discuss the asymptotic expansion for $\Delta\beta(nL)$. Just as for the energy, the Rydberg electron induces corrections to the Bethe logarithm for the $1s$ electron corresponding to the various multipole moments of the core, with the leading term being the dipole term $0.316\,205(6)\langle x^{-4}\rangle/Z^6$ [40, 41]. The complete expression is

$$\beta(1snl) = \beta(1s) + \left(\frac{Z-1}{Z}\right)^4 \frac{\beta(nl)}{n^3} + \frac{0.316\,205(6)}{Z^6}\langle x^{-4}\rangle + \delta_{\mathrm{ho}}\beta(1snl) \tag{29}$$

where the $\beta(nl)$ are hydrogenic Bethe logarithms [42], and $\delta_{\mathrm{ho}}\beta(1snl)$ takes into account contributions from the higher multipole moments. A least squares fit to direct calculations up to $L = 6$ and $n = 6$ for helium yields the results [43]

$$\delta_{\mathrm{ho}}\beta(1snl\ ^1\mathrm{L}) \quad = \quad 95.8(8)\langle r^{-6}\rangle - 845(19)\langle r^{-7}\rangle + 1406(50)\langle r^{-8}\rangle \tag{30}$$

Table 7: Residual two-electron Bethe logs $\Delta_{\rm ho}\beta(1snl)$.

State	$n^3\Delta\beta(1snl)$	Least squares fit	Difference
$3\,^1$D	–0.000 001 08(4)		
$3\,^3$D	0.000 181 74(5)		
$4\,^1$D	–0.000 018 4(3)		
$4\,^3$D	0.000 231 18(7)		
$5\,^1$D	–0.000 026 84(9)		
$5\,^3$D	0.000 249 73(12) [a]		
$4\,^1$F	0.000 006 58(2)	0.000 006 60	–0.000 000 02(2)
$4\,^3$F	0.000 007 63(2)	0.000 007 64	–0.000 000 01(2)
$5\,^1$F	0.000 008 70(3)	0.000 008 69	0.000 000 01(3)
$5\,^3$F	0.000 010 42(3)	0.000 010 41	0.000 000 01(3)
$6\,^1$F	0.000 009 8(1)	0.000 009 83	0.000 000 0(1)
$6\,^3$F	0.000 011 9(3)	0.000 011 98	–0.000 000 1(3)
$5\,^1$G	0.000 000 770(3)	0.000 000 770	0.000 000 000(3)
$5\,^3$G	0.000 000 771(3)	0.000 000 771	0.000 000 000(3)
$6\,^1$G	0.000 001 043(3)	0.000 001 042	0.000 000 001(3)
$6\,^3$G	0.000 001 050(8)	0.000 001 047	0.000 000 003(8)
$6\,^1$H	0.000 000 127(2)	0.000 000 127	0.000 000 000(2)
$6\,^3$H	0.000 000 127(2)	0.000 000 127	0.000 000 000(2)

[a] Corresponds to an energy uncertainty of ±14 Hz.

$$\delta_{\rm ho}\beta(1snl\ ^3{\rm L}) \;=\; 95.1(9)\langle r^{-6}\rangle - 841(23)\langle r^{-7}\rangle + 1584(60)\langle r^{-8}\rangle\,. \tag{31}$$

For example, for the $1s4f\ ^1$F state, $\beta(4\ ^1{\rm F}) = 2.984\,127\,1493(3)$. As can be seen from the comparison in Table 7, for higher L the asymptotic expansions reproduce the direct calculations to within the accuracy of the calculations.

The results as a function of Z can be represented by the $1/Z$ expansion

$$\beta(1sn\ell) = \frac{\beta(1s)+\beta(n\ell)/n^3}{1+\delta_{\ell,0}/n^3} + \frac{1}{n^3}\sum_{i=1}^{\infty}\frac{c_i}{Z^i} \tag{32}$$

The first few c_i coefficients can be estimated from a least-squares fit to the calculated values of $\beta(1sn\ell)$ up to $Z = 18$, resulting in the equations

$$\beta(1\,^1{\rm S}) \;=\; 2.984\,128\,556 - \frac{0.012315(23)}{Z} + \frac{0.02277(30)}{Z^2} + \frac{0.0019(7)}{Z^3}$$

$$\beta(2\,^1{\rm S}) \;=\; 2.964\,978\,525 + \frac{1}{8}\left(\frac{0.32744(66)}{Z} - \frac{0.1460(53)}{Z^2} - \frac{0.0019(7)}{Z^3}\right)$$

$$\beta(2\,^3{\rm S}) \;=\; 2.964\,978\,525 + \frac{1}{8}\left(\frac{0.22193(34)}{Z} - \frac{0.0099(25)}{Z^2} - \frac{0.0510(42)}{Z^3}\right)$$

Table 8: Comparison of Bethe Logarithms for lithium and its ions.

Atom	$Li(1s^2 2s)$	$Li(1s^2 3s)$	$Li^+(1s^2)$	$Li^{++}(1s)$
$\ln(k_0/Z^2 R_\infty)$	2.981 06(1)	2.982 36(6)	2.982 624	2.984 128

$$\beta(2\,^1\mathrm{P}) = 2.980\,376\,467 + \frac{1}{8}\left(\frac{0.0964(3)}{Z} - \frac{0.0940(26)}{Z^2} + \frac{0.022(4)}{Z^3}\right)$$

$$\beta(2\,^3\mathrm{P}) = 2.980\,376\,467 + \frac{1}{8}\left(\frac{0.0771(4)}{Z} - \frac{0.0395(37)}{Z^2} - \frac{0.017(6)}{Z^3}\right)$$

$$\beta(3\,^1\mathrm{S}) = 2.976\,397\,665 + \frac{1}{27}\left(\frac{0.5292(18)}{Z} - \frac{0.367(14)}{Z^2} + \frac{0.016(20)}{Z^3}\right)$$

$$\beta(3\,^3\mathrm{S}) = 2.976\,397\,665 + \frac{1}{27}\left(\frac{0.4296(3)}{Z} - \frac{0.1927(25)}{Z^2} + \frac{0.0425(43)}{Z^3}\right)$$

$$\beta(3\,^1\mathrm{P}) = 2.982\,714\,103 + \frac{1}{27}\left(\frac{0.1216(20)}{Z} - \frac{0.117(13)}{Z^2} + \frac{0.025(19)}{Z^3}\right)$$

$$\beta(3\,^3\mathrm{P}) = 2.982\,714\,103 + \frac{1}{27}\left(\frac{0.0992(11)}{Z} - \frac{0.0661(47)}{Z^2}\right)$$

The leading coefficient on the right-hand-side is just the quantity $(\beta(1s) + \beta(n\ell)/n^3)/(1 + \delta_{\ell,0}/n^3)$ from (32). These equations reproduce the directly calculated values to within the accuracy of the calculations. As a check, the leading c_1 terms inside parentheses for the low-lying states agree with the corresponding coefficients calculated by perturbation theory by Goldman and Drake [44] (see Ref. [38] for further details).

As a final remark, Table 8 compares the Bethe logarithms for the two lowest S-states of lithium with those for the Li-like ions $Li^+(1s^2\ ^1S)$ and $Li^{++}(1s\ ^2S)$. The comparison emphasizes again that the Bethe logarithm is determined almost entirely by the hydrogenic value for the $1s$ electron, and is almost independent of the state of excitation of the outer electrons, or the degree of ionization.

APPLICATIONS TO NUCLEAR SIZE MEASUREMENTS

As stated in the Introduction, one of the goals of this work is to use the comparison between theory and experiment for the isotope shift to determine the nuclear charge radius for various isotopes of helium and other atoms. One of the most interesting and important examples is the charge radius of the 'halo' nucleus ^{6}He. For a light atom such as helium, the energy shift due to the finite nuclear size is given to an excellent approximation by

$$\Delta E_{\mathrm{nuc}} = \frac{2\pi Z e^2}{3}\bar{r}_{\mathrm{c}}^2 \langle \sum_{i=1}^{2} \delta(\mathbf{r}_i) \rangle \tag{33}$$

where $\bar{r}_{\mathrm{c}}$ is the rms nuclear charge radius. If all other contributions to the isotope shift can be calculated to sufficient accuracy (about 100 kHz) and subtracted, then the residual shift due to the change in $\bar{r}_{\mathrm{c}}$ between the two isotopes can be determined from the measured isotope shift. The theory of isotope shifts, including

Table 9: Contributions to the ^{6}He - ^{4}He isotope shift (MHz).

Contribution	$2\,^3S_1$	$3\,^3P_2$	$2\,^3S_1 - 3\,^3P_2$
$\delta E_{\rm nr}$	52 947.324(19)	17 549.785(6)	35 397.539(16)
μ/M	2 248.202(1)	−5 549.112(2)	7 797.314(2)
$(\mu/M)^2$	−3.964	−4.847	0.883
$\alpha^2\mu/M$	1.435	0.724	0.711
$\delta E^{\rm a}_{\rm nuc}$	−1.264	0.110	−1.374
$\alpha^3\mu/M$, $E_{\rm L,1}$	−0.285	−0.037	−0.248
$\alpha^3\mu/M$, $E_{\rm L,2}$	0.005	0.001	0.004
Total	55 191.453(19)	11 996.625(4)	43 194.828(16)
Experiment[b]			43 194.772(56)
Difference			0.046(56)

[a]Assumed nuclear radius is $\bar{r}_{\rm c}(^6{\rm He}) = 2.04$ fm.
[b]Wang et al. [46].

relativistic recoil and radiative recoil contributions, is discussed in detail in Ref. [45], and will not be repeated here. Instead, we show as an example in Table 9 the various calculated contributions to the isotope shift for the $1s2s\ ^3S_1 - 1s3p\ ^3P_2$ transition of ^{6}He relative to ^{4}He. The corresponding experimental value was obtained in a remarkable experiment performed at the Argonne National Laboratory by Z.-T. Lu and collaborators [46], using the techniques of single-atom spectroscopy to trap the short-lived ^{6}He nuclei ($t_{1/2} = 0.8$ s) in the metastable $1s2s\ ^3S_1$ electronic state.

Each term in the table represents the energy difference between ^{6}He and ^{4}He with nuclear masses of 6.018 8880(11) u and 4.002 603 250(1) u respectively. The first entry $\delta E_{\rm nr}$ represents the 'normal' isotope shift due to the common mass scaling of all the nonrelativistic energies in proportion to $\mu/m_{\rm e} = 1 - \mu/M$, and the second entry is the 'specific' isotope shift due to mass polarization, calculated as a first-order perturbation. The remaining entries represent important corrections to these dominant terms. The third entry of order $(\mu/M)^2$ comes from second-order mass polarization, and the next term of order $\alpha^2\mu/M$ Ry is the relativistic recoil term. It contains contributions from the mass scaling of the terms in the Breit interaction, as well as cross-terms with the mass polarization operator, and the mass dependent Stone terms $(m_{\rm e}/M)(\tilde{\Delta}_2 + \tilde{\Delta}_{\rm so})$ in Eq. (13). The term $\delta E_{\rm nuc}$ is the finite nuclear size correction for an assumed nuclear charge radius $\bar{r}_{\rm c} = 2.04$ fm for ^{6}He, relative to the reference value $\bar{r}_{\rm c} = 1.673(1)$ fm for ^{4}He [47], [2] Finally, the two terms of order $\alpha^3\mu/M$ Ry denote the mass-dependent parts of the electron-nucleus ($E_{\rm L,1}$) and electron-electron ($E_{\rm L,2}$) QED shift, including recoil [50] and mass polarization corrections. The key point is that the uncertainty in the much larger mass-independent part of the QED shift (tens of MHz) cancels when the isotope shift is calculated. The residual uncertainty of only 16 kHz shown in Table 9 is then determined primarily by the uncertainty in the nuclear mass of ^{6}He, rather than the atomic physics calculations.

Since the goal of the experiment is to determine the nuclear charge radius for ^{6}He, the final step is to adjust $\bar{r}_{\rm c}$ so as to eliminate the small discrepancy of 0.046(56) MHz shown in Table 9. The various contributions to the isotope shift in Table 9 can be collected together and expressed in the form

$$\mathrm{IS}(2\,^3S - 3\,^3P) = 43\,196.202(16) + 1.008[\bar{r}_{\rm c}^2(^4{\rm He}) - \bar{r}_{\rm c}^2(^6{\rm He})] \qquad (34)$$

[2]This value is based on measurements of the Lamb shift in muonic helium, but attempts to reproduce the measurement have not proved successful, as discussed by Bracci and Zavattini [48]. The consistent, but less accurate value 1.676(8) fm has been obtained from electron scattering [49]. If the electron scattering value is used for ^{4}He, then the size of the error bars for the other helium isotopes increases in proportion, but the results do not otherwise change significantly.

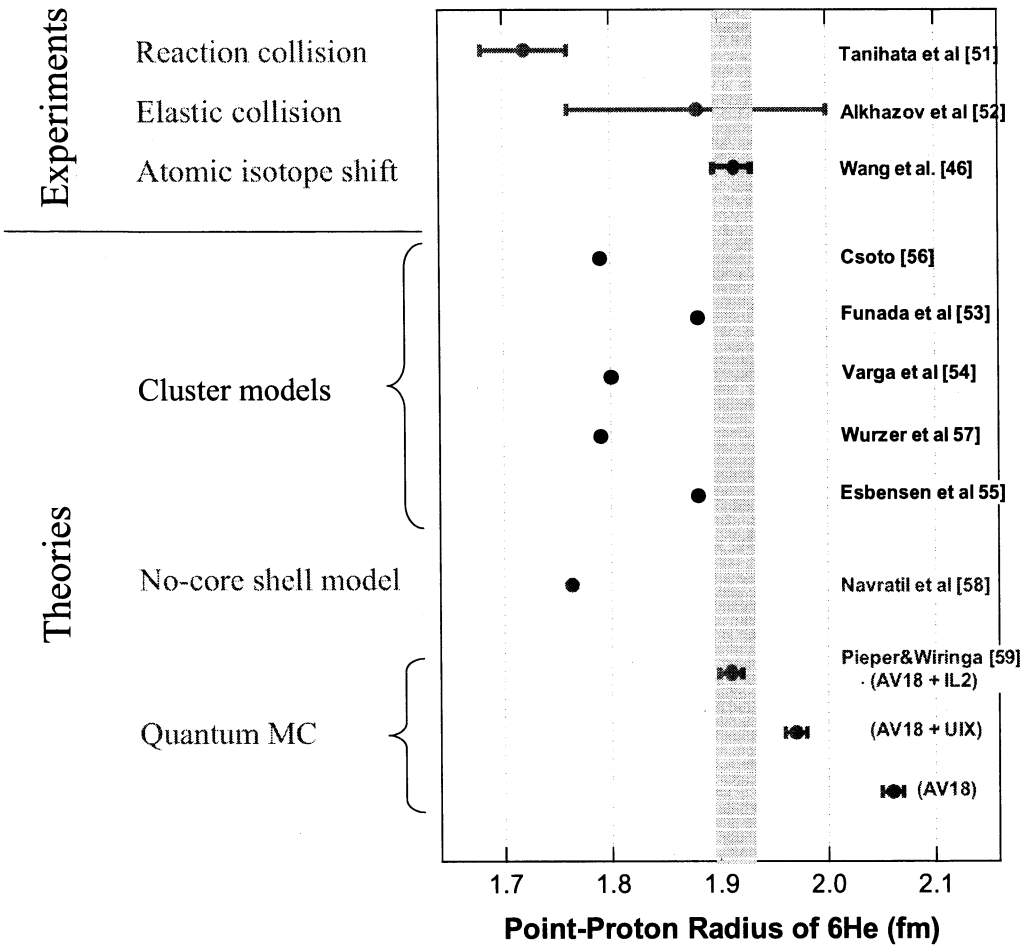

Figure 5: Comparison of the point-proton nuclear charge radius $\bar{r}_{\rm p}$ for ^{6}He with other measurements and theoretical values.

The adjusted nuclear charge radius is then $\bar{r}_{\rm c}(^6{\rm He}) = 2.054(14)$ fm.

The significance of this result in comparison with other measurements and calculations is illustrated in Fig. 5. [3] The first important point is that no other method of measurement is both independent of nuclear structure models, and capable of yielding sufficient accuracy to provide a meaningful test of theory. Ref. [53] was obtained from nuclear reaction cross sections, and Ref. [54] was extracted from elastic scattering from protons (in water). Second, the accuracy is sufficient to rule out all but two of the cluster calculations. Refs. [55, 56, 57] describe ^{6}He in terms of a single $(\alpha + {\rm n} + {\rm n})$ channel, but inclusion of the additional $({\rm t} + {\rm t})$ channel in Refs. [58, 59] produces a substantial disagreement. Also, the *ab initio* calculation based on the

[3]For comparison with theory, it is customary to express the calculated values in terms of an effective rms radius $\bar{r}_{\rm p}$ corresponding to a point-like proton and neutron, which is related to the rms charge radius $\bar{r}_{\rm c}$ by $\bar{r}_{\rm c}^2 = \bar{r}_{\rm p}^2 + \bar{R}_{\rm p}^2 + (N/Z)\bar{R}_{\rm n}^2$, where $\bar{R}_{\rm p} = 0.895(18)$ fm [51] is the rms charge radius of the proton, $\bar{R}_{\rm n}^2 = -0.116(5)$ fm^2 [52] is the mean-square charge radius of the neutron, and N and Z are the neutron and proton numbers.

no-core shell model [60] is in poor agreement. The best agreement is with the *ab initio* quantum Monte Carlo calculations of Pieper and Wiringa [61, 62] based on the AV18 two-body potential and the IL2 three-body potential, while other versions of the model potentials do not agree. The comparison with our value of $\bar{r}_c$ obtained by the isotope shift method is therefore capable of distinguishing amongst the various possible candidates for the effective low-energy nucleon-nucleon interaction potential.

SUMMARY AND CONCLUSIONS

The principle message of this paper is that the helium atom and other quantum mechanical three-body systems can be solved essentially exactly for all practical purposes in the nonrelativistic limit, and there is a systematic procedure for calculating the relativistic and other higher-order QED corrections as perturbations. The solution of the problem of calculating Bethe logarithms means that the theoretical energy levels are complete up to and including terms of order α^3 Ry. Both Aaron Temkin and Richard Drachman have had a profound influence on the field through their study of variational methods and electron scattering phenomena. As shown here, Drachman's asymptotic expansion methods are of key importance in extending the variational results to cover the entire spectrum of singly-excited states. In fact, the accuracy of the asymptotic expansion method increases so rapidly with increasing L that variational calculations become completely unnecessary for $L > 7$.

As a consequence of these advances, helium now joins the ranks of hydrogen and other two-body systems as examples of fundamental atomic systems. The high precision theory that is now available creates new opportunities to develop measurement tools that would otherwise not exist. One such example discussed here is the determination of the nuclear charge radius for the halo nucleus ^{6}He. This opens up a new area of study at the interface between atomic physics and nuclear physics, and it provides important input data for the determination of effective nuclear forces. Other similar experiments have been performed on the lithium isotopes [63], including the halo nucleus ^{11}Li [64], and further work is in progress on ^{8}He at Argonne and ^{11}Be at GSI/TRIUMF.

ACKMOWLEDGMENTS

I would like to express my gratitude to Richard Drachman and Aaron Temkin for many interesting and stimulating discussions over the years, and for the leadership they have provided to the field. In the words of Joe Sucher, the have helped to "slay the dragon of atomic physics." I would also like to thank Wilfried Nörtershäuser at GSI and Z.-T. Lu at the Argonne National Laboratory for their hospitality and inspiration on the experimental side, and Zong-Chao Yan who has contributed tremendously to the calculations, especially for lithium. This work was supported by the Natural Sciences and Engineering Research Council of Canada.

REFERENCES

1. G.W.F. Drake and W.C. Martin, Can. J. Phys. **76**, 597 (1998).
2. I. Tanihata, Nucl. Phys A **522**, C275 (1991).
3. B. Klahn and W.A. Bingel. Theor. Chem. Acta, **44**, 27 (1977); Int. J. Quantum Chem. **11**, 943 (1978).
4. G.W.F. Drake and Z.-C. Yan. Phys. Rev. A, **46**, 2378 (1992).

5. G.W.F. Drake, in *Long-range Casimir forces: Theory and recent experiments on atomic systems*, edited by F.S. Levin and D.A. Micha (Plenum, New York, 1993), pp. 107–217.

6. G.W.F. Drake, Adv. At. Mol. Opt. Phys. **31**, 1 (1993).

7. G.W.F. Drake, M.M. Cassar, and R.A. Nistor, Phys. Rev. A **65**, 054501 (2002).

8. A.K. Bhatia and A. Temkin, Phys. Rev. **137**, 1335 (1965).

9. A.K. Bhatia and R.J. Drachman, Phys. Rev. A **35**, 4051 (1987).

10. A.K. Bhatia and R.J. Drachman, J. Phys. B: At. Mol. Opt. Phys. **36**, 1957 (2003).

11. V.I. Korobov, Phys. Rev. A **66**, 024501 (2002).

12. C. Schwartz, http://xxx.aps.org/abs/physics/0208004.

13. S.P. Goldman, Phys. Rev. A **57**, R677 (1998).

14. A. Bürgers, D. Wintgen, J.-M. Rost, J. Phys. B: At. Mol. Opt. Phys. **28**, 3163 (1995).

15. J.D. Baker, D.E. Freund, R.N. Hill, J.D. Morgan III, Phys. Rev. A **41**, 1247 (1990).

16. R.J. Drachman, Phys. Rev. A **26**, 1228 (1982).

17. R.J. Drachman, Phys. Rev. A **31**, 1253 (1985).

18. R.J. Drachman, Phys. Rev. A **33**, 2780 (1986).

19. R.J. Drachman, Phys. Rev. A **37** 979 (1988).

20. R.J. Drachman, Phys. Rev. A **47**, 694 (1993).

21. R. J. Drachman, in *Long-Range Casimir Forces: Theory and Recent Experiments on Atomic Systems*, edited by F. S. Levin and David Micha (Plenum Press, New York, 1993), pp. 219–272, and earlier references therein.

22. R.A. Swainson and G.W.F. Drake, Can. J. Phys. **70**, 187 (1992).

23. Z.-C. Yan and G.W.F. Drake, Phys. Rev. Lett. **81**, 774 (1998).

24. Z.-C. Yan and G.W.F. Drake, Phys. Rev. A, **66**, 042504 (2002).

25. Z.-C. Yan and G.W.F. Drake, Phys. Rev. Lett., **91**, 113004 (2003).

26. A.K. Bhatia and R.J. Drachman, Phys. Rev. A **45** 7752 (1992).

27. R.J. Drachman and A.K. Bhatia, Phys. Rev. A **51** 2926 (1995).

28. A.K. Bhatia and R.J. Drachman, Phys. Rev. A **55**, 1842 (1997).

29. H.A. Bethe and E.E. Salpeter, *Quantum mechanics of one- and two-electron atoms*, (Springer-Verlag, New York, 1957).

30. A.P. Stone, Proc. Phys. Soc. (London) **77**, 786 (1961); **81**, 868 (1963).

31. P. K. Kabir and E. E. Salpeter, Phys. Rev. **108**, 1256 (1957).

32. H. Araki, Prog. Theor. Phys. **17**, 619 (1957).

33. J. Sucher, Phys. Rev. **109**, 1010 (1958).

34. C. Schwartz, Phys. Rev. **123**, 1700 (1961).

35. J. D. Baker, R. C. Forrey, J. D. Morgan III, R. N. Hill, M. Jeziorska, and J. Schertzer, Bull. Am. Phys. Soc. **38**, 1127 (1993); J. D. Baker, R. C. Forrey, M. Jeziorska, and J. D. Morgan III, private communication.

36. V. I. Korobov and S. V. Korobov, Phys. Rev. A **59**, 3394 (1999).

37. K. Pachucki and J. Sapirstein, J. Phys. B: At. Mol. Opt. Phys. **33**, 455 (2000).

38. G.W.F. Drake and S.P. Goldman, Can. J. Phys. **77**, 835 (1999).

39. V.I. Korobov, Phys. Rev. A **69**, 054501 (2004).

40. S.P. Goldman and G.W.F. Drake, Phys. Rev. Lett. **68**, 1683 (1992).

41. S.P. Goldman, Phys. Rev. A **50**, 3039 (1994).

42. G. W. F. Drake and R. A. Swainson, Phys. Rev. A **41**, 1243 (1990).

43. G.W.F. Drake, Phys. Scr. T95, 22 (2001).

44. S. P. Goldman and G. W. F. Drake, J. Phys. B: At. Mol. Opt. Phys. **17**, L197 (1984).

45. G.W.F. Drake, W. Nörtershäuser, and Z.-C. Yan, Can. J. Phys. 83, 311 (2005).

46. L.-B. Wang, P. Mueller, K. Bailey et al. Phys. Rev. Lett. 93, 142501 (2004).

47. E. Borie and G.A. Rinker, Phys. Rev. A **18**, 324 (1978).

48. L. Bracci and E. Zavattini, Phys. Rev. A **41**, 2352 (1990).

49. I. Sick, Phys. Lett. B 116, 212 (1982).

50. K. Pachucki and J. Sapirstein, J. Phys. B **33**, 455 (2000).

51. I. Sick, Phys. Lett. B **576**, 62 (2003).

52. S. Kopecky, P. Riehs, J.A. Harvey and N.W. Hill, Phys. Rev. Lett. **74**, 2427 (1995); S. Kopecky, J.A. Harvey, N.W. Hill, M. Krenn, M. Pernicka, P. Riehs and S. Steiner, Phys. Rev. C **56**, 2229 (1997).

53. I. Tanihata et al., Phys. Lett. B **289**, 261 (1992).

54. G.D. Alkhazov et al., Phys. Rev. Lett. **78**, 2313 (1997).

55. S. Funada, H. Kameyama and Y. Sakruagi, Nucl. Phys. **A575**, 93 (1994).

56. K. Varga, Y. Suzuki and Y. Ohbayasi, Phys. Rev. C **50**, 189 (1994).

57. H. Esbensen, G.F. Bertsch and K. Hencken, Phys. Rev. C **56**, 3054 (1997).

58. A. Csoto, Phys. Rev. C **48**, 165 (1993).

59. J. Wurzer and H.M. Hofmann, Phys. Rev. C **55**, 688 (1997).

60. P. Navratil, J.P. Vary, W.E. Ormond and B.R. Barrett, Phys. Rev. Lett. **87**, 172502 (2001).

61. S.C. Pieper, V.R. Pandharipande, R.B. Wiringa and J. Carlson, Phys. Rev. C **64**, 014001 (2001).

62. S.C. Pieper and R.B. Wiringa, Ann. Rev. Nucl. Part. Sci. 51, 53 (2001).

63. G. Ewald, W. Nörtershäuser, A. Dax, S. Göte, R. Kirchner, H.-J. Kluge, Th. Kühl, R. Sanchez, A. Wojtaszek, B.A. Bushaw, G.W.F. Drake, Z.-C. Yan, and C. Zimmermann, Phys. Rev. Lett. **93**, 113002 (2004); **94**, 039901 (2005).

64. R. Sanchez, W. Nörtershäuser, G. Ewald, D. Albers, J. Behr, P. Bricault, B.A. Bushaw, A. Dax, J. Dilling, M. Dombsky, G.W.F. Drake, S. Gotte, R. Kirchner, H.J. Kluge, T. Kühl, J. Lassen, C.D.P. Levy, M.R. Pearson, E.J. Prime, V. Ryjkov, A. Wojtaszek, Z.-C. Yan and C. Zimmermann, Phys. Rev. Lett. **96**, 033002 (2006).